

## Fatigue performance assessment of welded joints using the infrared thermography

J.L. Fan<sup>\*1,2</sup>, X.L. Guo<sup>1</sup> and C.W. Wu<sup>1</sup>

<sup>1</sup>State Key Laboratory of Structural Analysis for Industrial Equipment, Dalian University of Technology, Dalian 116024, China

<sup>2</sup>School of Mechanical Engineering, Department of Mechanical Engineering, Purdue University, West Lafayette, IN 47906, USA

(Received September 1, 2011, Revised October 12, 2012, Accepted October 24, 2012)

**Abstract.** Taking the superficial temperature increment as the major fatigue damage indicator, the infrared thermography was used to predict fatigue parameters (fatigue strength and  $S-N$  curve) of welded joints subjected to fatigue loading with a high mean stress, showing good predictions. The fatigue damage status, related to safety evaluation, was tightly correlated with the temperature field evolution of the hot-spot zone on the specimen surface. An energetic damage model, based on the energy accumulation, was developed to evaluate the residual fatigue life of the welded specimens undergoing cyclic loading, and a good agreement was presented. It is concluded that the infrared thermography can not only well predict the fatigue behavior of welded joints, but also can play an important role in health detection of structures subjected to mechanical loading.

**Keywords:** fatigue performance; welded joint; infrared thermography; energetic damage model; residual fatigue life

---

### 1. Introduction

The durability of welded components is governed by the strong interactions among different influencing factors such as loading histories, residual stresses and complex weld geometries. Thus, a great number of fatigue failures can still take place at crucial welded details even though a relatively low dynamic stress is cyclicly applied on high-strength steels for design purposes. Over all, it is valuable and interesting to carry out experimental research on the relationship between the fatigue performance and the static tensile strength due to the increasing use of high-strength steels in practical engineering.

At present, four main evaluation methods for fatigue assessment are commonly used in practical applications: 1) Nominal stress method; 2) Hot-spot stress method; 3) Notch stress method; 4) Linear elastic fracture mechanics (Hobbacher 2009). The fatigue strength (fatigue class FAT) of welded joints is defined as the stress level at  $2 \times 10^6$  cycles of the  $S-N$  curve in accordance with the current guidelines of the International Institute of Welding (IIW) (International Institute of Welding

---

\*Corresponding author, Ph.D., E-mail: fanjunling@mail.dlut.edu.cn

1996). It is based on the nominal stress and the hot-spot stress that the first two methods are able to be applied to determine fatigue parameters of welded joints. Nevertheless, they meet some unavoidable limitations in practical engineering designs (Fricke 2003): the nominal stress is impossible to be decided in critical components with complex geometries; the selection of FAT is subjective due to the effects of the joint geometries and the loading histories on the fatigue responses; the hot-spot stress is significantly affected by the local stress at the welds with complex properties, which is strongly dependent on the finite element models; the size effect and the thickness effect are neglected during the analysis of the hot-spot stress method in order to simplify the processing procedures. The influence of the local weld on the fatigue responses is able to be taken into account by the notch stress method, and the parameterized formula is derived using the finite element analysis (FEA) by idealizing the shape of the weld toe. It is sensitive to the crack size for the linear fracture mechanics method. The residual fatigue life of components with small cracks can be well predicted by use of the Paris theory, whereas the computational requirement is fairly greater than that needed in other methods. In addition, the fracture mechanics method is not suitable to determine the crack initiation life.

The infrared thermography, as a full-field, non-destructive, real-time and non-contact technique, makes it possible to overcome the above limitations of the traditional procedures and to give good predictions of fatigue parameters (Boulanger *et al.* 2004, Luong 2007). It was first applied to assess fatigue limits of materials with a stepwise loading procedure (La Rosa and Risitano 2000), and to establish the entire *S-N* curve with a limited number of specimens (Fargione *et al.* 2002, Fan *et al.* 2012).

Materials and mechanical components, undergoing cyclic loads, are subjected to an increase of the surface temperature since the fatigue damage is a process of the mechanical energy dissipation. The surface temperature, measured by an infrared camera, is tightly associated with the fatigue responses of materials and components. In the research carried out by Guo *et al.* (2011), a good agreement was achieved between the traditional results and the predicted results by applying the infrared thermographic methodology on welded joints. Crupi *et al.* (2009, 2010) investigated the applications of the infrared thermography on high-cycle fatigue tests and low-cycle fatigue tests, and accordingly a linear correlation between the stabilized hysteresis energy and the asymptotic temperature increment was found. It is an experimental fact that the mechanical energy dissipates into the surrounding mainly as heat energy. The higher the temperature at the hottest zone on the specimen surface, the higher the applied cyclic stress level. Based on this experimental fact, Risitano *et al.* (2010) proposed and developed a new damage model using the infrared thermography to predict the cumulative damage due to the previous loading histories. Furthermore, experimental tests were carried out by Clienti *et al.* (2010) to confirm that the static test coupled with the thermographic analysis was able to provide reliable information about the thermoelastic limit. Ummenhofer and Medgenberg (2009) improved the infrared thermography to study the local plastic deformations for the fatigue damage evaluation during fatigue loading.

In this paper, an application of the infrared thermographic methodology for predicting fatigue parameters of welded joints subjected to a high mean stress is presented to verify its validity and to extend its capabilities. The temperature evolution of the hot-spot zone on the welded joint surface during the fatigue test was used to analyze the fatigue damage status related to safety evaluation. Resorting to the energy theory, an energetic damage model was established to predict the residual fatigue life of welded joints.

## 2. Theoretical background

### 2.1 The infrared thermography (TM)

In the published papers (Fargione *et al.* 2002, Luong 2007), it is reported that the coupled thermomechanical equations are the theoretical basis of the infrared thermography. The temperature increment of metallic materials and mechanical components, subjected to fatigue loading lower than the yield limit  $\sigma_s$  but higher than the endurance limit  $\sigma_f$ , appears to rapidly increase at the beginning of the fatigue test. After that a relatively stationary value is reached within only few cycles. The higher the applied cyclic stress level, the higher the stationary temperature value. The stationary temperature is closely related to the fatigue behavior of materials and components. As a result of that, it is widely used to evaluate the fatigue limit and the damage status. It is experimentally confirmed that the temperature change induced by the cyclic stress level below  $\sigma_f$  is negligible in comparison with that due to the stress above  $\sigma_f$ . That is mainly attributed to the minor influence of non-plastic effects (e.g., viscosity effect and anelasticity effect) on the fatigue damage (Luong 2007). In literature (Crupi *et al.* 2009, 2010, Fan *et al.* 2011), a good linear relationship between the stationary temperature increment  $\Delta T_s$  and the cyclic stress range squared  $\Delta\sigma^2$  was presented to predict the fatigue limit of components. As a consequence, the fatigue limit  $\sigma_f$ , related to the physical phenomenon, is defined as the highest stress level causing no temperature increment. This means that fatigue limit  $\sigma_f$  can be obtained by extrapolating the regression line down to zero at the  $\Delta\sigma^2$ -axis.

In practical operation, in order to obtain the stationary temperature increments  $\Delta T_s$  with only one specimen, a stepwise loading procedure, from the lowest stress to the highest stress, is applied on the same specimen at the same loading frequency.

### 2.2 The energy theory

The infrared thermography, based on a successive loading procedure, enables us to determine the whole  $S$ - $N$  curve of materials and components by using theoretically only one specimen. Fatigue fracture takes place once the energy dissipated per unit volume reaches a threshold value  $E_c$  (the limiting energy per unit volume) which is independent of the loading conditions (Clienti *et al.* 2010, Risitano *et al.* 2010).  $E_c$  introduced by Risitano *et al.* (2010) is documented to be proportional to the energetic parameter  $\Phi$  which can be calculated by integrating the  $\Delta T$ - $N$  curve recorded by an infrared camera.

$$E_c \propto \Phi = \int_0^{N_f} \Delta T(N) \cdot dN \quad (1)$$

Where  $N_f$  denotes the final fatigue life. In a simple form, the energetic parameter  $\Phi$  can be obtained by the following equation since the surface temperature almost remains the same after the initial temperature rise

$$\Phi = \Delta T_s \cdot N_f \quad (2)$$

A succession of increasing loads, at the same frequency, is stepwise applied to the same specimen for a fixed number of cycles. The stationary temperature values  $\Delta T_{s,i}$ , corresponding to the applied stress ranges  $\Delta\sigma_{a,i}$ , are obtained by means of an infrared camera. Accordingly, the energetic constant

$\Phi$  can be an average value by testing a set of specimens. And subsequently, the relevant fatigue life  $N_{fi}$  is readily determined. The fatigue  $S$ - $N$  curve can be plotted directly on the set of couples  $(\Delta\sigma_{ai}, N_{fi})$  based on the energy approach.

### 2.3 The energetic damage model

It is of interest and importance to predict the residual fatigue life of components subjected to cyclic loading. Based on the effective energy dissipation, Xuan *et al.* (1997) established a non-linear damage accumulation law, considering the different loading sequences. Using the theory of the plastic hysteresis energy, Wu (1994) investigated the fatigue damage status of aluminium alloy undergoing random fatigue loading, and the residual fatigue life was well predicted with a nonlinear damage model. Using the energy theory, the energetic damage model will be advanced to predict the relevant residual fatigue life of welded joints.

The damage of a material or a component after  $n_i$  cycles with the cyclic stress range  $\Delta\sigma_i$  is

$$D_i = \frac{n_i}{N_{fi}} \quad (3)$$

Where  $N_{fi}$  denotes the entire fatigue life under the cyclic stress range  $\Delta\sigma_i$ .

As a consequence, the Miner's law can be written as

$$D = \sum_{i=1}^j \frac{n_i}{N_{fi}} = 1 \quad i = 1, 2, 3, \dots, j \quad (4)$$

Where  $j$  is the total number of stress levels.

Based on the energy accumulation theory, the damage accumulation rate can be expressed by use of the energy accumulation rate as follow

$$D_i = \frac{n_i}{N_{fi}} = \frac{\Delta W_i n_i}{E_c} \quad (5)$$

Where  $\Delta W_i$  is the stable hysteresis energy per cycle, and  $E_c$  denotes the limiting energy.

Under the adiabatic condition, Crupi (2008) derived the relationship between the stable hysteresis energy and the stationary temperature increment by neglecting the influence of heat conduction, convection and radiation

$$\Delta W_i = \frac{\rho C_p \Delta T_{si}}{N_{si}} \quad (6)$$

Where  $\rho$  denotes the material density;  $C_p$  is the specific heat capacity;  $N_{si}$  is the cycle number when the stationary temperature increase  $\Delta T_{si}$  is reached at the beginning of the fatigue test.

The limiting energy can be calculated by

$$E_c = \Delta W_i \cdot N_{fi} = \frac{\rho C_p \Phi}{N_{si}} \quad (7)$$

Substituting Eqs. (6) and (7) into Eq. (5), the expression of the fatigue damage model is derived as

$$D_i = \frac{n_i}{N_{fi}} = \frac{\Delta T_{si} \cdot n_i}{\Phi} \quad (8)$$

Thus, the expression of the energetic damage model resorting to the energy theory can be written as

$$D = \sum_{i=1}^k \frac{\Delta T_{si} \cdot n_i}{\Phi} = 1 \quad i = 1, 2, \dots, k \quad (9)$$

In this paper, the cycle number  $n_i$  is equal to the cycle number  $N_{si}$  after the surface temperature tends to be a stationary value. With the energy model above, the residual fatigue life can be predicted rapidly.

### 3. Materials and methods

#### 3.1 Material and specimen

The material, used for the experimental tests, is martensite stainless steel 630 according to ASTM

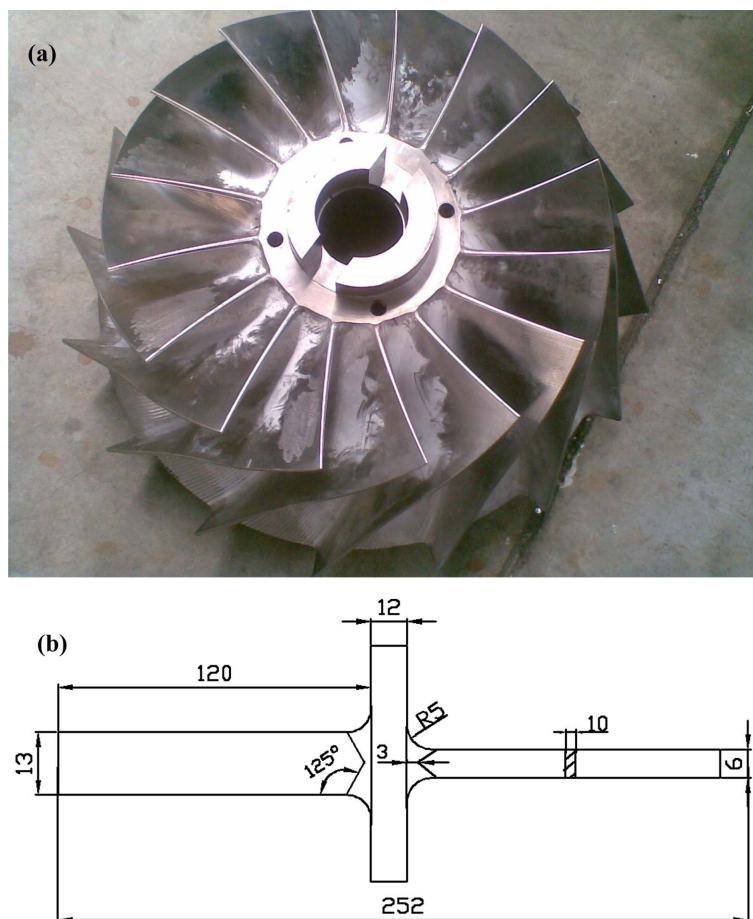


Fig. 1 (a) Impeller, (b) size of the welded joint (unit: mm)

Table 1 Chemical composition of steel 630 (w, %)

C	Si	Mn	P	S	Ni	Cr	Cu	Nb	Mo
0.02-0.07	0.15-0.70	0.3-1.0	≤0.03	≤0.0025	5.0-6.0	13.0-14.5	1.3-1.8	0.25-0.45	1.3-1.8

Table 2 The heat treatment processes

Type of the heat treatment	Conditions	Holding time
Solution Treatment	1050 ± 10°C, air-cooling	1.5-2.5 h
Thermal Refining Treatment	850 ± 10°C, oil-cooling	1.5-2.5 h
Aging Treatment	480 ± 10 C, air-cooling	2.0-3.0 h

Table 3 Mechanical properties of 630 steel

Tensile strength $\sigma_p$ (MPa)	Yield strength $\sigma_{p0.2}$ (MPa)	Elastic modulus (GPa)	Elongation after fracture (%)
1309	1080	202	40

AISI designation, which is widely used in impeller blades presented in Fig. 1(a). It was first smelt by alkaline electric arc furnace, and then the electroslag refining (ESR) was performed (Fan *et al.* 2012). The nominal chemical compositions of the steel are listed in Table 1, and its mechanical properties, after a set of heat treatments presented in Table 2, were experimentally evaluated and are reported in Table 3. The cruciform welded joints, as shown in Fig. 1(b), were machined using the manual arc-welding technique. To improve the mechanical properties of welded joints, the post-welding heat treatments following Table 2 were carried out.

### 3.2 Experimental methods

Before experimental tests, the surfaces of the welded joints should be polished using a fine grit paper in order to decrease the stress concentration due to the surface effects, and then be painted black to decrease the IR reflection and to get a greater thermal radiation.

Fatigue tests were carried out at room temperature by using a fully computerized MTS810 system servo-hydraulic machine with a 100 kN capacity as shown in Fig. 2. Fatigue tests were conducted by applying a fixed nominal mean stress level  $\sigma_m = 640$  MPa to consider the centrifugal force caused by the high speed rotation of impeller blades. It is worth noting that the loading mode differs from the previous work with a fixed stress ratio. The nominal stress ranges  $\Delta\sigma_a$ , in a sinusoidal waveform with a frequency of 18 Hz, are in the range of 160–400 MPa. The infinite fatigue life was defined as 5 million cycles. If fatigue fracture did not occur within the specific cycle number, the fatigue test was suspended and that only happened for the nominal stress ranges lesser than 140 MPa. In the present paper, 32 specimens were tested in order to reasonably describe the fatigue behavior of cruciform welded joints. Due to the scattering feature of the fatigue data, especially for the welded components significantly affected by the thermal welding process, the mathematical statistical method must be used to analyze the experimental results.

Furthermore, fatigue test was performed by applying the successive loading procedure on the same specimen (La Rosa and Risitano 2000). The nominal stress ranges started from 140 MPa with steps of 20 MPa every 60000 cycles in order to decrease the fatigue damage accumulation. During

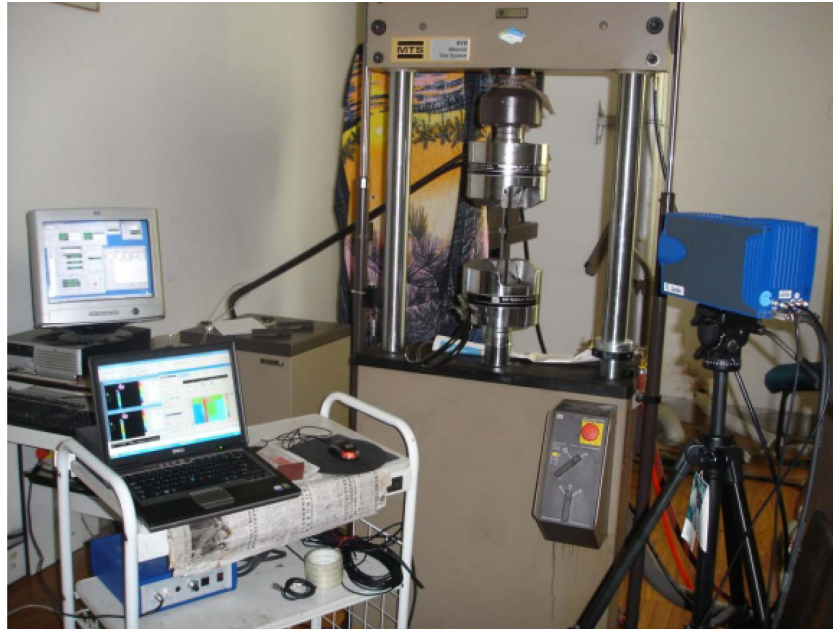


Fig. 2 Experimental system

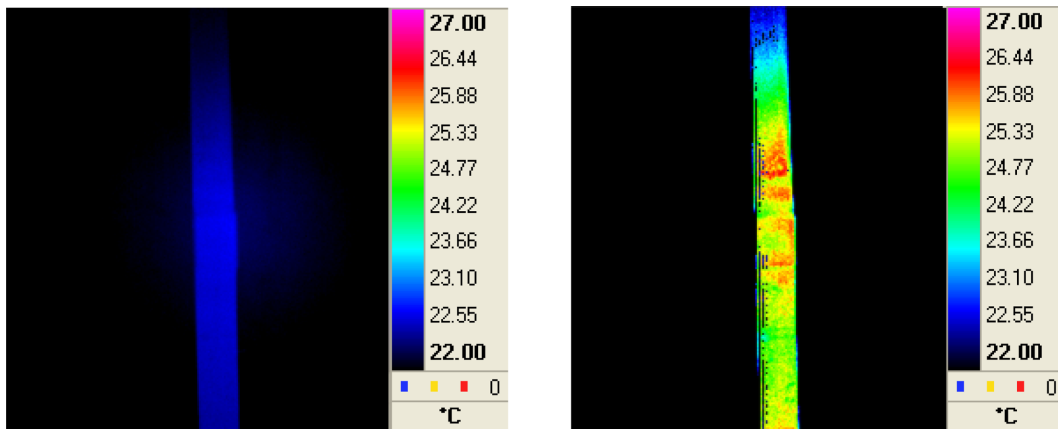


Fig. 3 Thermal images of a welded specimen ( $\Delta\sigma = 250$  MPa) in the early (left) and final (right) stage

the fatigue tests, the Cedip Jade III infrared camera, located at 1m in front of the tested specimens, was applied to record the surface temperature  $T(t)$  of the welded joints and the surrounding temperature  $T_0$ . The thermal images, presented in Fig. 3, were captured by means of Altair software containing  $320 \times 240$  pixels.

#### 4. Results and discussion

All the fractured welded joints failed in the weld toe zone due to the complex material properties



Fig. 4 The fractured specimen

and high stress concentrations. The typical fatigue features of the fractured specimens are presented in Fig. 4. The fatigue tests, conducted by using the infrared system, enable us to obtain the following results:

- 1)  $S-N$  curves at 50% and 97.7% survival probabilities;
- 2) Fatigue parameters obtained by the traditional  $S-N$  curves;
- 3) Fatigue parameters predicted by the infrared thermography and the energy method;
- 4) Fatigue damage evaluation by use of the hot-spot evolution;
- 5) Comparison between the predicted results and the traditional results.

#### 4.1 The traditional test results

To well understand the fatigue behavior of the welded joints, the statistical analysis was used to describe the fatigue data with a power function

$$\Delta\sigma^m N_f = C \quad (10)$$

Where  $\Delta\sigma$  is the stress range;  $N_f$  is the fatigue life;  $m$  and  $C$  are material constants. This is the  $S-N$  curve with 50% survival probability called the median  $S-N$  curve (ASTM 2004).

A linear equation can be derived by expressing  $\Delta\sigma$  and  $N_f$  as the logarithm form

$$\log(N_f) = -m\log(\Delta\sigma) + \log(C) \quad (11)$$

As a consequence, the material constants  $m$  and  $C$  are able to be obtained by employing the least-square method.

The  $S-N$  curve with a higher survival probability (usually 97.7% for welded joints) is able to be presented by calculating the standard deviation of the remaining samples since  $\log(N_f)$  is considered to be a normal distribution (i.e., Gaussian distribution).

The  $S-N$  curves, at different survival probabilities  $P_s = 50\%$  and  $P_s = 97.7\%$ , are shown in Fig. 5. The fatigue strength at 2 million cycles (i.e., fatigue class FAT) and the fatigue limit at 5 million cycles are accordingly determined by extrapolating the  $S-N$  curve down to the specific cycle number. Moreover, the slopes of the two  $S-N$  curves are the same due to  $\log(N_f)$  normally distributed. The higher the survival probabilities, the lower the fatigue limits.

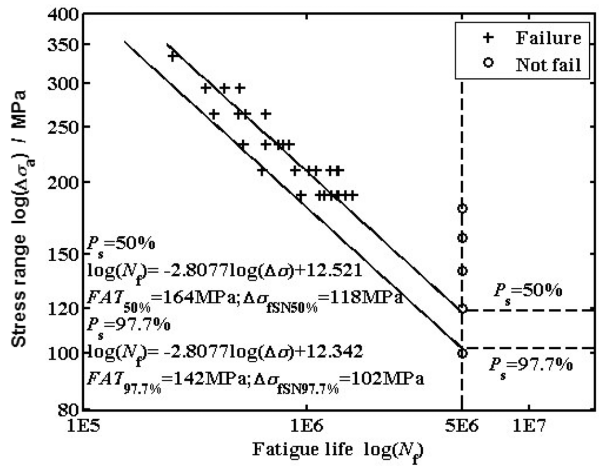


Fig. 5 S-N curves by the traditional method in bi-logarithmic scale

4.2 Fatigue parameters obtained using the infrared technique

In the present paper, the differential thermographic technique was applied to calculate the surface temperature increment  $\Delta T_s$  for the purpose of avoiding any errors resulted from the environmental perturbation and the limited sensitivity of the experimental system.

$$\Delta T_s = T(t) - T_0 \tag{12}$$

where  $T(t)$  is the surface temperature of the specimen, and  $T_0$  is the surrounding temperature.

The detailed process of the differential thermographic method is schematically presented in Fig. 6. Resorting to the stepwise loading procedure, all the stationary temperature increase  $\Delta T_s$  corresponding to the applied stress range level  $\Delta\sigma$  is able to be determined using the thermographic method mentioned above.

Fig. 7 shows the  $\Delta T$ - $N$  curves at different nominal stress ranges  $\Delta\sigma_{ai}$ . The surface temperature becomes almost stationary before reaching the first 40000 cycles which is negligible compared with the whole fatigue life. It is obviously observed that the  $\Delta T$ - $N$  curves take on typical three phases.

Based on the infrared thermography, the surface temperature increments of the welded specimens are conveniently obtained by a successive fatigue tests at the increasing stepwise loading. Fig. 8

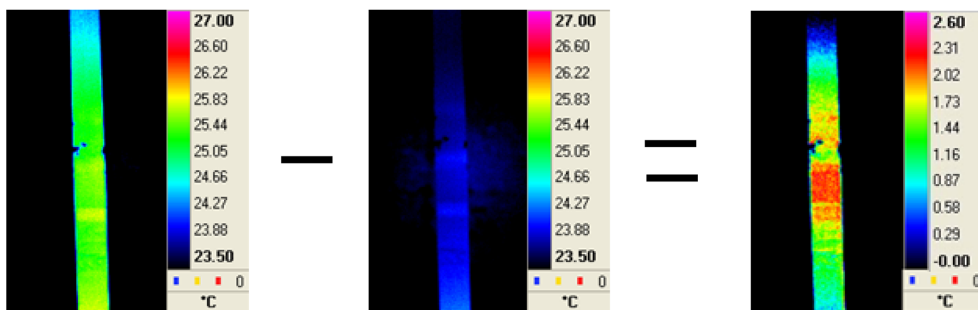


Fig. 6 The differential thermographic method

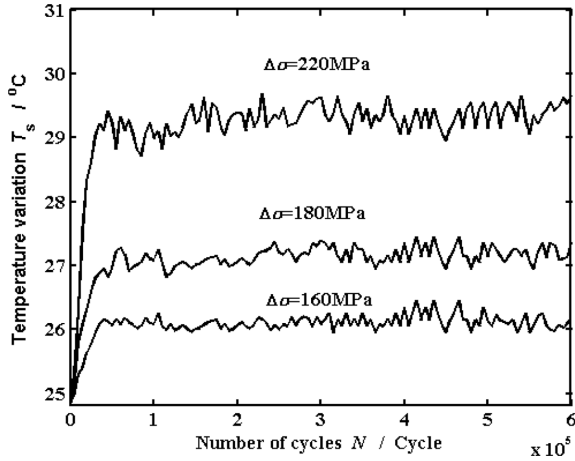


Fig. 7  $\Delta T$ - $N$  curves at different nominal stress ranges

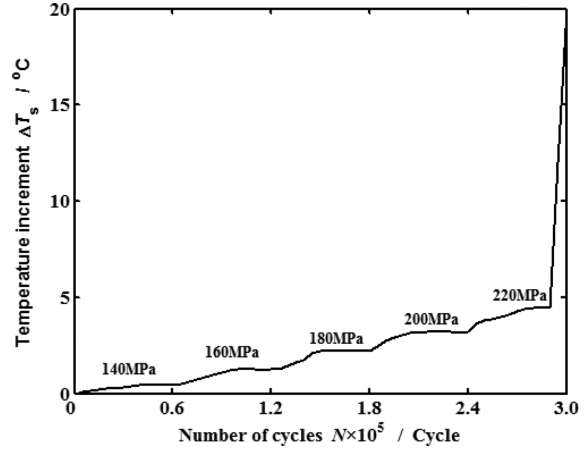


Fig. 8  $\Delta T$ - $N$  curve by the successive stepwise loading procedure

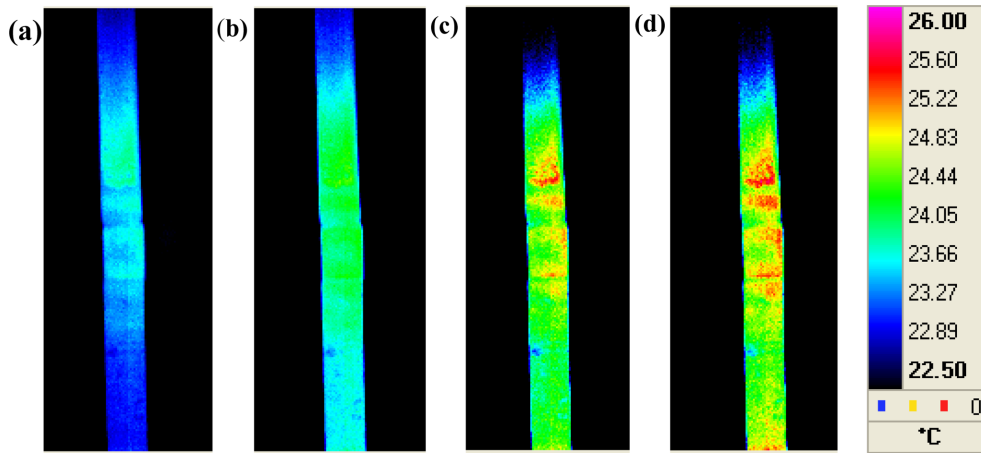


Fig. 9 Hot-spot zone at different nominal stress ranges (a) 140 MPa, (b) 160 MPa, (c) 180 MPa, (d) 200 MPa

shows one  $\Delta T$ - $N$  curve of the welded joints tested. As it is seen, the higher the cyclic stress ranges  $\Delta\sigma_{ai}$ , the higher the temperature increments  $\Delta T_{si}$ . Fig. 9 presents the thermographic images of the hottest zone on the specimen surface at the increasing cyclic loading during a successive loading procedure. With the fatigue damage evolution, the hottest zone starts to expand gradually due to the localized plastic deformation induced by the increasing loads. The variations of the surface temperature field enable us to qualitatively identify the damage status which is quite useful for safety evaluation of structures in service.

The thermographic data, i.e., the stationary temperature increment  $\Delta T_s$ , was directly associated with the corresponding stress range squared  $\Delta\sigma^2$ . A regression line (as presented in Fig. 10) using the least-square method was readily plotted based on the couples  $(\Delta T_s, \Delta\sigma^2)$ . As a consequence, the fatigue limit was determined as 123 MPa by extrapolating the regression line down to zero at the  $\Delta\sigma^2$ -axis.

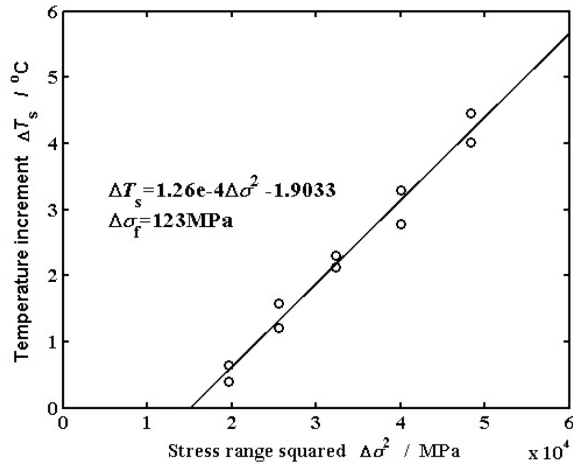


Fig. 10 The infrared thermography

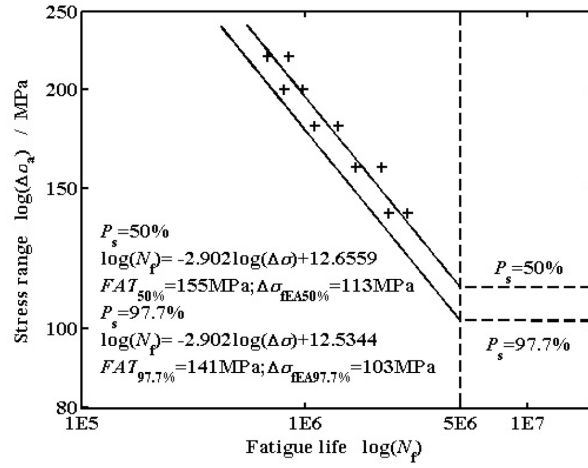


Fig. 11 The S-N curve predicted by the energy method

Table 4 Comparison of the fatigue parameters ( $P_s = 50\%$ )

Method	FAT (MPa)	$\delta\%$	$\Delta\sigma_f$ (MPa)	$\delta\%$
The traditional method	164	-	118	-
The energy method	155	5.5%	113	4.2%
The infrared methodology	-	-	123	4.2%

Resorting to the energy method, the whole S-N curves, at different survival probabilities  $P_s = 50\%$  and  $P_s = 97.7\%$ , were determined based on the infrared thermography, as presented in Fig. 11. It is clearly shown that the material constants  $m = 2.9021$  and  $C = 12.6559$  are in good agreement with the ones given in Fig. 5 obtained by the traditional testing method.

To demonstrate the good predictions of the infrared thermographic methodology, the fatigue parameters  $\Delta\sigma_{fSN}$  obtained by the traditional procedures were compared with the predicted values  $\Delta\sigma_{fp}$  assessed by the infrared thermography and the energy method. Table 4 is the comparison between  $\Delta\sigma_{fSN}$  and  $\Delta\sigma_{fp}$ . Note that the errors between the predicted values and the traditional results are less than 10%. It is concluded that the infrared thermography enables us to well predict the fatigue parameters of welded joints subjected to fatigue loading even though a high mean stress level  $\sigma_m = 640$  MPa is applied on the welded components. The differences between the fatigue limits are possibly attributed to the interactions among the definitions themselves and the scattering feature of the fatigue data along with the limited sensitivity of the testing system. Assuming that the shape of the S-N curve above 1 million cycles is the same (Crupi *et al.* 2009), the traditional fatigue limit  $\Delta\sigma_{fSN}$  is defined as the stress level corresponding to 5 million cycles. But the fatigue limit  $\Delta\sigma_{fp}$ , predicted by the infrared thermography, is considered as the highest cyclic stress level causing no temperature increment. It is considered that the stress below  $\Delta\sigma_{fp}$  will cause no fatigue damage accumulation during the fatigue evolution process. In a word, from the stand point of the physical phenomenon, the infrared thermography, as a mature technique in fatigue research, takes more actual factors into account to overcome the strong objectivity of the traditional testing method.

Table 5 Comparison between the energetic damage model ( $P_s = 50\%$ )

	$\Delta\sigma_{a1}$ (MPa)	$\Delta T_{s1}$ (°C)	$N_1$	$\Delta\sigma_{a2}$ (MPa)	$\Delta T_{s2}$ (°C)	Predicted life	Actual life	Errors
#1	180	1.95	450000	220	3.89	335100	378296	11.4%
#2	220	3.73	300000	180	2.07	513062	597431	14.1%

#### 4.3 The residual life prediction by the energetic damage model

In this part, two welded specimens, undergoing two cyclic stress levels with different loading sequences, were tested to confirm the capability of the energetic damage model in predicting the residual fatigue life. The two sinusoidal stress ranges were, respectively, 180 MPa and 220 MPa, and the surface temperature increments were real-timely recorded by an infrared camera.

Table 5 presents the detailed testing processes. The errors between the predicted values by the energetic damage model and the actual values are less than 15%, achieving a good prediction. That confirms that the fatigue responses of materials and components are more or less affected by the loading sequences. The possible reason is that the crack density rapidly increases under the high-low loading sequence (Xuan *et al.* 1997). By contrast, this phenomenon is not obviously observed. Through the application of the energetic damage model, it is concluded that the model not only gives accurate predictions of the residual fatigue life, but also presents a clear physical meaning from the view of the energy accumulation.

## 5. Conclusions

The infrared thermography, as a promising technique, enables us to assess the fatigue limit of welded joints along with the whole  $S-N$  curve by using a limited number of specimens in a very short time, and good predictions of fatigue limits and fatigue strength are achieved even though a high mean stress is applied in order to take into account the real operating situations during the fatigue tests. Moreover, the  $S-N$  curves with adequate survival probabilities can be predicted by calculating the standard deviation of the remaining samples.

The hottest zone on the specimen, subjected to fatigue loading, is the critical location related to the final fatigue fracture. The surface temperature variation here, recorded by an infrared camera, is able to be used to evaluate the fatigue damage status which is useful for safety evaluation.

The energetic parameter  $\Phi$ , independent of the loading sequences, is a constant value related to material properties. Based on the limiting energy  $E_c$  which is proportional to the energetic parameter  $\Phi$ , the residual fatigue life of the welded joint is able to be determined, and a good prediction is presented with the actual value. The energetic damage model exhibits a clear physical meaning from the view of the energy accumulation during the fatigue process.

## Acknowledgements

The financial supports of Natural Science Foundation of China (No.11072045), National Basic Research Program of China (No.2011CB706504) and China Scholarship Council are gratefully

acknowledged. Moreover, I would also like to thank Thomas Siegmund, Professor of Department of Mechanical Engineering of Purdue University in USA, for supporting the research work at Purdue University.

## References

- ASTM E 739-91 (2004), "Standard practice for statistical analysis of linear or linearized stress-life ( $S-N$ ) and strain-life ( $\varepsilon-N$ ) fatigue data", *ASTM*.
- Boulanger, T., Chrysochoos, A., Mabru, C. and Galtier, A. (2004), "Calorimetric analysis of dissipative and thermoelastic effects with the fatigue behavior of steels", *Int. J. Fatigue*, **26**, 221-229.
- Clienti, C., Fargione, G., La Rosa, G., Risitano, A. and Risitano, G. (2010), "A first approach to the analysis of fatigue parameters by thermal variations in static tests on plastics", *Eng. Fract. Mech.*, **77**, 2158-2167.
- Crupi, E., Guglielmino, V., Maestro, M. and Marino, A. (2009), "Fatigue analysis of butt welded AH36 steel joints: thermographic method and design S-N curve", *Mar. Struct.*, **22**, 373-386.
- Crupi, V., Chiofalo, G. and Guglielmino, E. (2010), "Using infrared thermography in low-cycle fatigue studies of welded joints", *Weld. J.*, **89**, 195-200.
- Crupi, V. (2008), "An unifying approach to assess the structural strength", *Int. J. Fatigue*, **30**, 1150-1159.
- Fan, J.L., Guo, X.L., Wu, C.W. and Zhao, Y.G. (2011), "Research on fatigue behavior evaluation and fatigue fracture mechanisms of cruciform welded joints", *Mater. Sci. Eng. A*, **528**, 8417-8427.
- Fan, J., Guo, X. and Wu, C. (2012), "A new application of the infrared thermography for fatigue evaluation and damage assessment", *Int. J. Fatigue*, **44**, 1-7.
- Fan, J., Guo, X., Wu, C. and Deng, D. (2012), "Effect of heat treatments on fatigue properties of FV520B steel using infrared thermography", *Chin J. Mater. Res.*, **26**, 61-67. (in Chinese)
- Fargione, G., Geraci, A., La Rosa, G. and Risitano, A. (2002), "Rapid determination of the fatigue curve by the thermographic method", *Int. J. Fatigue*, **24**, 11-19.
- Fricke, W. (2003), "Fatigue analysis of welded joints: state of development", *Mar. Struct.*, **16**, 185-200.
- Guo, X.L., Fan, J.L. and Zhao, Y.G. (2011), "Fatigue behavior analysis of cruciform welded joints by infrared thermographic method", *Adv. Mater. Res.*, **197-198**, 1395-1399.
- Hobbacher, A.F. (2009), "The new IIW recommendations for fatigue assessment of welded joints and components – A comprehensive code recently updated", *Int. J. Fatigue*, **31**, 50-58.
- International Institute of Welding (1996), "Fatigue design of welded joints and components Abington Cambridge", *Abington Publishing*, UK.
- La Rosa, G. and Risitano, A. (2000), "Thermographic methodology for rapid determination of the fatigue limit of materials and mechanical components", *Int. J. Fatigue*, **22**, 65-73.
- Luong, M.P. (2007), "Introducing infrared thermography in soil dynamics", *Infrar. Phys. Techn.*, **49**, 306-311.
- Risitano, A. and Risitano, G. (2010), "Cumulative damage evaluation of steel using infrared thermography", *Theor. Appl. Fract. Mec.*, **54**, 82-90.
- Ummenhofer, T. and Medgenberg, J. (2009), "On the use of infrared thermography for the analysis of fatigue damage processes in welded joints", *Int. J. Fatigue*, **31**, 130-137.
- Wu, F.M. (1994), "Estimation of fatigue life under random loading with plastic hysteresis energy theory", *Chinese J. Aeronautics*, **7**, 289-294.
- Xuan, F.Z., Sun, S.X., Tang, H.W. and Cheng, D.M. (1997), "Effective energy dissipation analysis method for fatigue damage of laminated composites", *Acta Mater. Compos. Sin.*, **14**, 115-124. (in Chinese)